

Milestone SP3B6DM4
Results of Gravity Modeling of the Paleozoic Basement
30 January 1998

Principle Investigator - Ernest L. Majer
Lane R. Johnson, D. W. Vasco, Paul Parker

*Ernest Orlando Lawrence Berkeley National Laboratory
Berkeley, California 94720*

1 Scope and Purpose of the Report

In 1996 a study of the surface geophysics at Yucca Mountain and vicinity was submitted as Milestone OB05M (Majer et al. 1996). Included in that report was a section on the collection and interpretation of surface gravity. When the project was originally planned it was anticipated that the gravity data would be used primarily as a constraint on the interpretation of the seismic reflection data. However, the seismic lines were not successful in achieving sufficient depth of penetration to reliably image basement structure, so it became necessary to place more dependence upon the gravity data as a means of developing a model of the basement structure in the vicinity of Yucca Mountain. Thus included in Milestone OB05M (Majer et al. 1996) was a model of depth to basement based on a trial-and-error interpretation of the gravity data. This model was obtained by fixing the density contrast between the Cenozoic deposits and the Paleozoic basement and then varying the depth to basement to achieve general agreement between the long wavelength components of the calculated and observed gravity anomalies.

The purpose of the study reported in this milestone is to provide a reinterpretation of the gravity data in terms of basement structure which incorporates some standard methods of geophysical inverse theory. This should help to diminish some of the subjectivity that is always present in trial-and-error fittings of observational data and at the same time provide some crude estimates of the uncertainty of the model.

However, an important fact that applies to the results of both this and the previous milestone is that the interpretation of surface gravity data by itself is inherently nonunique. The methods reported in this milestone can not remove this fundamental nonuniqueness, but can only hope to quantify it.

2 Background

The equipment, acquisition procedures, reduction procedures, and general properties of the gravity data are all described in Milestone OB05M (Majer et al. 1996) and will not be repeated here. As described in Milestone OB05M (Majer et al. 1996), LBNL collected gravity data along 17 linear profiles in the vicinity of Yucca Mountain. In addition, as also described in Milestone OB05M (Majer et al. 1996), the coverage of the gravity data was extended by including data from a United States Geological Survey (USGS) digital gravity catalog for the Nevada Test Site (NTS). The final results were presented in terms of Bouguer gravity anomalies in that milestone report and these same anomalies provide the starting point for the interpretation presented in the current milestone.

3 Parameterization of the Model and Data

The study concentrated on basement depth in the region between 36.8 and 36.9 N latitude and between 116.5 and 116.4 W longitude, which is an area roughly 11 by 9 km approximately centered on the proposed repository. For the purposes of the inversion this area was divided into 400 rectangular cells 0.005 degrees on a side (0.55 by 0.44 km). The average depth to basement within each of these cells was regarded as a model parameter which could vary in the inversion. The density contrast between the Cenozoic deposits and the Paleozoic basement was fixed at the value used in Milestone OB05M (Majer et al. 1996), which was nominally 0.27 g/cm^3 .

The same 400 rectangular cells which were used to parameterize the model were used to parameterize the observed gravity data. All of the LBNL gravity observations that fell within a given cell were averaged to yield a single mean value for that cell. When more than one observation was available for a cell the standard error of the

mean was also calculated to provide a measure of the uncertainty. In cells where only one observation was available, a standard error of the mean of 0.1 mgal was used, which is commensurate with estimates of the data precision given in Milestone OB05M (Majer et al. 1996). Following this procedure, estimates of observed gravity were obtained for 105 of the 400 cells.

The digital gravity catalog of the USGS was used to augment the observed gravity data. A procedure similar to that used for the LBNL data was used except it was required that more than one observation per cell be present and that the standard error of the mean either be less than 0.1 mgal or less than one half the residual gravity anomaly. This procedure produced observed gravity values for 22 additional cells that were not sampled by the LBNL data.

The basic inverse problem consisted of estimating the depth to basement in 400 cells based on gravity observations in either 105 or 127 cells, depending upon whether only the LBNL data or combined LBNL and USGS data were used.

4 Solution of the Inverse Problem

Two different procedures for solving the inverse problem were employed, a conjugate gradient method and a genetic algorithm method. The conjugate gradient method begins with an initial model and uses a descent procedure to find another model which improves the fit between observed and calculated gravity data. The method is quite effective in finding an improved model, but there is no assurance that this is the global minimum in the objective function. The genetic algorithm method has some of the characteristics of the Monte Carlo method and thus has a better chance of finding a global minimum in the objective function. Both methods were used in this study in an attempt to partially characterize some of the basic non-uniqueness that was anticipated to be in the results.

Both methods of inversion require a procedure for calculating gravity anomalies for arbitrary models of basement structure. All of these calculations were performed with the same basic procedure used in Milestone OB05M (Majer et al. 1996), which is based on the method of Johnson and Litehiser (1972) for integrating the gravitational attraction of three dimensional bodies described in a spherical coordinate system. Whereas in the previous milestone this method was used to calculate the attraction of large bodies with dimensions of several km, in the present milestone it is used to

calculate the attraction of a large number of small bodies with lateral dimensions of less than a km. A numerical check was performed to compare the calculated values of a single large cell with dimensions of 0.1 degree by 0.1 degree and that same area divided into 400 small cells. The two calculations agreed to within 0.001 mgal, which is well below the precision of the observed gravity data.

5 Inversions with Conjugate Gradient Method

Our primary goal is to find a model of basement topography compatible with our gravity observations. However, it is well known that some degree of non-uniqueness is inevitable in such a geophysical inverse problem (Parker, 1994). That is, there will be a set, possibly infinite, of models which fit the observations within their estimated errors. We approach the inherent ambiguity in two ways: regularizing the inverse problem and presenting multiple models. We shall describe the procedures in more detail below.

First, we consider the method for determining basement depths compatible with our observations and describe our approach for regularizing the inverse problem. The fit to the data, $\mathcal{F}(\mathbf{x})$, is measured in a composite sense as the sum of the squares of the M gravity residuals,

$$\mathcal{F}(\mathbf{x}) = \sum_{i=1}^M r_i^2(\mathbf{x}) \quad (1)$$

where \mathbf{x} is the vector of N model parameters (basement depths) and the i -th residual, $r_i(\mathbf{x})$, is given by the observed minus the predicted gravity anomaly. Predicted anomalies are generated using an integration technique based upon the work of Johnson and Litehiser (1972). In general, the misfit functional is augmented by one or more penalty terms. These additional terms represent model characteristics which are thought to be undesirable. For example, extremely large variations from our initial model of basement structure (which already fit the data quite well) might not be expected. One measure of the size of basement variation from the initial model is the sum of the squares of the deviations,

$$\mathcal{A}(\mathbf{x}) = \sum_{i=1}^N (x_i - x_i^p)^2 = (\mathbf{x} - \mathbf{x}^p)^T \cdot (\mathbf{x} - \mathbf{x}^p) \quad (2)$$

where \mathbf{x}^p is a prior model of basement structure. A penalized misfit functional, $\mathcal{P}(\mathbf{x})$, incorporating the above ideas is given by

$$\mathcal{P}(\mathbf{x}) = \sum_{i=1}^M r_i^2(\mathbf{x}) + c_a(\mathbf{x} - \mathbf{x}^p)^T \cdot (\mathbf{x} - \mathbf{x}^p) \quad (3)$$

where c_a is the weighting coefficient for the model norm penalty term.

There are a number of ways to minimize $\mathcal{P}(\mathbf{x})$ based upon local linearizations about some initial basement structure, \mathbf{x}_0 (Gill, Murray, and Wright, 1981). In our experience the Fletcher-Reeves variant of the conjugate gradient algorithm (Gill, Murray, and Wright, 1981; Press et al. 1989) has proven to be efficient and robust. Briefly, the conjugate gradient routine requires an initial model, \mathbf{x}_0 , which is successively updated in an additive fashion,

$$\mathbf{x}_{k+1} = \mathbf{x}_k + \alpha_k \mathbf{p}_k \quad (4)$$

where the scalar α_k is determined by a one-dimensional minimization in the direction of \mathbf{p}_k . The vector \mathbf{p}_k is given by the formula

$$\mathbf{p}_k = -\mathbf{g}_k + \beta_{k-1} \mathbf{p}_{k-1} \quad (5)$$

where

$$\beta_{k-1} = \frac{\|\mathbf{g}_k\|^2}{\|\mathbf{g}_{k-1}\|^2}$$

and

$$\mathbf{g}_k = \nabla \mathcal{P}(\mathbf{x}_k).$$

The gradient is recomputed after each line search and the algorithm is periodically restarted for each cycle of conjugate vectors, \mathbf{g}_k .

Our starting model, which is also our prior model, is shown in Figure 1. It is the end result of combining geological information and gravity observations to produce a large scale model of basement structure around the repository, as described in Milestone OB05M (Majer et al. 1996). In this report we are attempting to refine this structure, examining basement variations for the region shown in Figure 1. The large scale basement structure was sub-divided into a 20 (latitude) by 20 (longitude) grid of prismatic elements. In Figure 1, we have interpolated the prism depths onto a 100 by 100 grid for plotting purposes. The values shown in Figure 1 are depth to basement from sea level in kilometers. The horizontal and vertical coordinates are distances

in feet from an origin of $X_0 = 549,464.67$ feet, $Y_0 = 781,757.57$ feet, Nevada state plane coordinates. The star signifies the location of well P1 which encountered the basement. The thin line denotes the outline of the proposed repository.

There were two main categories of data used in this study: qualified observations gathered by Berkeley Laboratory and unqualified observations made previously by the USGS. For the most part our qualified observations are restricted to accessible roads in the area and are limited in areal distribution. The USGS data augment our measurements in spatial coverage but appear to be contaminated by greater error. For the purposes of this report we performed two groups of inversions for basement structure, those without USGS measurements and those with the observations.

All basement topography models described in this section were obtained using the conjugate gradient algorithm outlined above. Twenty conjugate gradient iterations were used in all inversions. After 15 iterations the solutions did not change significantly. The model norm penalty was used to regularize the inversion and weighting values (c_a , equation 3) of 1 and 3 are shown below. Our choice of weighting was based upon a series of inversions using 9 different values of c_a , each a factor of 3 larger than the other. In this fashion we could explore how the size of the basement variations and the fit to the data varied with c_a . For example, consider Figure 2 which is a plot of the sum of squares of the depth deviations from the prior model versus squared error (misfit). We seek solutions which fit the data but do not have excessive basement variations, as measured by the model norm, equation (2). The values of $c_a = 1, 3$ appear to span the range of models which satisfy these objectives. Solutions associated with these penalty weightings are shown in Figure 3. Also shown in this figure are the gravity residuals with respect to the prior basement model (Figure 1), the gravity signal which is not explained by the prior model. These models of basement structure are based solely on Berkeley Laboratory qualified data. Models of basement depth based upon both Berkeley Laboratory and USGS data are shown in Figure 4.

6 Inversions with Genetic Algorithm Method

Genetic algorithms (Goldberg, 1989) are global nonlinear optimization methods based on principles of Darwinian natural selection. There are several advantages in using a genetic algorithm for this particular problem. First, a genetic algorithm search is more likely to find a global minimum than gradient based methods if the minimum

is hidden among many local minima, and second, the search is unbiased in terms of the starting model. Genetic algorithms search with a certain amount of randomness in order to avoid a poor solution in a local minima, but they are actually quite exploitative, processing a vast amount of information in parallel in order to efficiently mix the optimal parameters and find a global solution.

The algorithm we used to invert for the basement structure follows that presented in Goldberg (1989). Solving problems with a standard genetic algorithm involves the following six steps:

1. Generating an initial population of random (binary) strings which will represent a population of models.
2. Decoding the binary strings into floating point models and evaluating the fitness of each model with an objective function.
3. Subjecting the models to a selection process in order to weed out models with poorly performing parameters.
4. Crossover between the selected models in order to mix desirable characteristics.
5. Occasional random mutation in order to insure that no information is permanently lost in the crossover operation.
6. Overwriting the old generation and going back to step (3) for as many generations as desired.

In the initial coding of the problem, a search space is designated. The search is unbiased within the space because the initial population of models is selected randomly from the model space. As with the conjugate gradient inversion, the basement structure was subdivided into a 20×20 grid of prismatic elements. Each of the 400 floating point model parameters was represented by a binary string of 8 bits in length, giving an accuracy of 1 part in 256. An initial population of 150 models was generated randomly to sample the search space, which was determined by varying the prior model depths by $\pm 30\%$ and ± 1 km. The minimum value of a parameter was

$$x_i^{min} = x_i^o - 0.3x_i^o - 1.0$$

and its maximum value was

$$x_i^{max} = x_i^o + 0.3x_i^o + 1.0$$

The inversion was performed for 127 station points (which includes the LBNL and the USGS data). After 150 generations (22500 objective function evaluations) the algorithm converged to a misfit of 26.9 mgals² from the prior model misfit of 60.7 mgals² (Figure 5), or an average of 0.46 mgal misfit per station. The genetic algorithm inversion result is shown in Figure 6.

There is no smoothness constraint or regularization applied to the genetic algorithm inversion, and the inversion appears to be somewhat unstable, especially in regions with sparse station coverage. However, the result provides an unbiased complement to the inversion carried out with the conjugate gradient method.

7 QA Status of Data and Codes

Two sets of gravity data were employed to derive the basement models presented here. The primary data was gathered by Berkeley Laboratory as described in Milestone OB05M (Majer et al. 1996) and has been QA'ed. These data were used to derive the models in Figures 3a and 3b. In order to improve spatial coverage additional USGS data was included in the additional inversions shown in Figures 4a, 4b, and 6. The USGS data were only used to provide corroborating evidence and the conclusions of this report do not depend on these data.

Both the conjugate gradient and genetic algorithms depend on the gravity calculations of the forward code. The forward code, the code to calculate gravity given a model of basement depth variation, has been QA'ed during the previous Milestone OB05M. The conjugate gradient algorithm used here is from software distributed with the book Numerical Recipes (Press et al. 1989). A description of the code may be found in that text (p. 301-307). The program is a non-linear least squares statistical fitting routine which is exempt under the QA program. The genetic algorithm functions much like a Monte Carlo routine in that it repeatedly calls the forward routine, a form of trial and error. The essential difference is that the genetic algorithm combines models based upon their fit to the observed data. The genetic algorithm program used in this report is currently undergoing QA evaluation. The genetic algorithm only provided an independent collaboration of results based upon the conjugate gradient algorithm. That is, the results of our report do not depend on the model provided by the genetic algorithm.

8 Results

All of the depth to basement models obtained with the formal inversion procedures fit the observed gravity data better than the initial model, which was the model presented in Milestone OB05M (Majer et al. 1996). In terms of an objective function, here taken to be the sum of squares of the gravity residuals, the fit was between 2 and 4 times better. This type of improvement is in agreement with expectations. Correspondingly, the models obtained with the formal inversion procedures (Figures 3a, 3b, 4a, 4b, and 6) were more complex than the very smooth initial model (Figure 1). This too is to be expected, as the inversion procedures are capable of finding the combinations of small perturbations in depth which provide an optimum fit to the data.

It appears that the regularization which was used in the conjugate gradient method does not play a dominant role in determining the model. This can be ascertained by comparing Figure 3a with Figure 3b and by comparing Figure 4a with Figure 4b, with the latter member of each pair having 3 times as much regularization as the first. The models obtained with more regularization are somewhat smoother than those with less regularization in each case, but the differences in general are small and the major features in the basement topography are quite similar in all of the models. With respect to regularization, a comparison can also be made with the model obtained with the genetic algorithm model (Figure 6), which contained no regularization. This model shows the most variation of all, with many short wavelength features present in the basement topography, but it is also apparent that a smoothed version of this model contains the same major features present in the models obtained with the conjugate gradient method.

Adding the unqualified data from the USGS digital gravity catalog helps improve the data coverage for the Yucca Mountain site and does not appear to have any negative effects upon the general model. This conclusion is based on a comparison of Figures 3 and 4. The models in Figure 4 show a few extra basement features in areas where new observational data has been added, but in the areas where qualified data were already present the changes in basement structure are minimal. As with the case of regularization, the major features in basement topography do not appear to be critically dependent upon whether only qualified data or augmented data were used in the inversion.

An evaluation of the relative merits of the results obtained with the conjugate gradient method and the genetic algorithm method is rather difficult in the present case, as the strengths and weaknesses of the two methods are complimentary. As

stated above, it appears that a smoothed version of the genetic algorithm results contains the same major features present in the conjugate gradient results (compare Figure 6 and Figure 4b), but this is somewhat of a subjective judgment. There are some major differences in the computational effort involved in the two methods, as the genetic algorithm method typically takes a few days for a single inversion on a workstation, whereas the conjugate gradient method only takes a few minutes to hours on the same workstation.

The only point in this model where depth to basement is actually known is at well P1. This depth was not constrained in any of the inversions so that it could be used as a check on any bias that might be present in the results. The conjugate gradient inversions with both LBNL and USGS data yielded depths of 0.13 km below sea level for the basement at P1, whereas the genetic algorithm inversion yielded a depth of 0.30 km with the same data. The initial model had a depth of 0.20 km. Thus, at least at this single check point, the inversions appear to be producing reasonable results. Another check on the results is the consistency of the gravity derived basement models with estimates from seismic reflection data. The results from the gravity inversions in Figures 3b and 4b are shown in Figure 7 as a cross section along the regional seismic line REG-3 of Brocher et al. (1996). The Common Depth Points (CDP) locations are shown at the top of the figure. Also shown are the new interpretations to top of Pz from Feighner et al. (1998) based on the P1 VSP analysis. Shown are the two different interpretations (one shallow and one deep) to the top of the Pz. In general, the shallow Pz pick is more consistent with the gravity results near the P1 borehole, showing the Pz to be relatively flat lying here. The shallow Pz pick also matches the gradient seen in the gravity results between CDP's 440-560; however, the fit diverges beneath Yucca Mountain, possibly due to the uncertainties in the velocity model used to depth convert REG-3.

A number of models of basement structure in the vicinity of Yucca Mountain based on surface gravity measurements have been obtained with two different formal inversion methods. It is important to assess which of the features in these models are actually required by the observational data, and thus likely to be actually present in the basement structure, and which are artifacts related to the inversion procedure. A complete assessment of this type is not possible, but a reasonable approach is to regard the features in basement structure which are common to all of the models as the features which are the most reliable. Always keeping in mind the basic nonuniqueness of results of this type, those features appear to be the following:

- The shallowing of the basement in a west to east direction under Yucca Moun-

tain, which was present in the initial model, is still present in all of the inversion models. It has been altered somewhat, with more of a north-south strike than the initial southwest-northeast strike and a steeper gradient in some of the models.

- The shallow horst structure in the vicinity of drill hole P1 which was present in the initial model persists, but it has developed an extension toward Yucca Mountain in a northwest direction in the inversion models. This feature extends under the southern end of the proposed repository.
- The deepening of the basement in a south to north direction, which was a simple step in the basement in the initial model, is present in all of the inversion models, but it has been changed into a more gradual north dipping feature with some variations along its strike.
- The step in the basement down into Crater Flat in the vicinity of Solitario Canyon which was contained in the initial model has not been changed much in the inversion models, partly because of the small amount of observational data available to constrain this part of the model.

References

- Brocher, T.M., Hart P.E., Hunter W.C. , and Langenheim V.E. 1996, Hybrid-source Seismic Reflection Profiling across Yucca Mountain, Nevada: Regional Lines 2 and 3, *USGS Open File Report -96-28*, MOL.19970310.0094, GS960108314211.002 (Q), USGS, Denver, Colorado, 110.
- Feighner M.A., Daley T.M., Gritto R., and Majer E.L. 1998, Results of VSP Analysis in P1, *Yucca Mountain Project Milestone SP3B6AM4*, Lawrence Berkeley National Laboratory, Berkeley, California, DTN: LB980130123112.001 (Q).
- Gill, P. E., W. Murray, and M. H. Wright, 1981. *Practical Optimization*, Academic Press, London.
- Goldberg, D.E., 1989. *Genetic Algorithms in Search, Optimization, and Machine Learning*, Addison-Wesley, Reading, MA.
- Johnson, L. R., and J. J. Litehiser, 1972. A method for computing the gravitational attraction of three-dimensional bodies in a spherical or ellipsoidal Earth, *J. Geophys. Res.*, **77**, 6999-7009.
- Parker, R. L., 1994. *Geophysical Inverse Theory*, Princeton University Press, Princeton.
- Press, W. H., B. P. Flannery, S. A. Teukolsky, and W. T. Vetterling, 1989. *Numerical Recipes*, p. 301, Cambridge University Press, Cambridge.
- Majer, E. L., Feighner M., Johnson L., Daley T., Karageorgi E., Lee K.H., Williams K., and McEvelly T. 1996, Synthesis of Borehole and Surface Geophysical Studies at Yucca Mountain, Nevada and Vicinity Volume I: Surface Geophysics, *Yucca Mountain Project Milestone OB05M*, Lawrence Berkeley National Laboratory, Berkeley, California, DTN: LB960808314212.001 (Q), LB960808314212.002 (Q), LB960808314212.003 (Q), LB960808314212.004 (Q), ACCN: MOL.19970114.0137.

Figure Captions

- Figure 1.** Prior model of basement depth variations. Depths with respect to sea level are indicated by the color scale. The star denotes the location of well P1, the thin line outlines the proposed repository.
- Figure 2.** Curve portraying the variation of the fit to the gravity observations (sum of the squares of the gravity residuals) and the size of the basement deviations (sum of the squares of the differences between the model depths and the prior model depths) from the prior model as a function of the weighting coefficient c_a in equation (3). The points 1 and 3 signify models in which the norm weighting coefficient had the values 1 and 3, respectively.
- Figure 3.** Inversion results based upon Berkeley Laboratory data only. The gravity residuals used to derive the models are also indicated in these figures. The size of each square is proportional to the difference between the observed gravity and the gravity predicted by the prior model in Figure 1. Fill squares indicate positive residuals while open squares indicate negative residuals. The two panels correspond to two values of c_a in equation (3). WEIGHT=1 corresponds to $c_a = 1$ and WEIGHT=3 corresponds to $c_a = 3$.
- Figure 4.** Inversion results based upon a joint inversion of Berkeley Laboratory and USGS data. The gravity residuals used to derive the models are also indicated in these figures. The two panels correspond to two values of c_a in equation (3). WEIGHT=1 corresponds to $c_a = 1$ and WEIGHT=3 corresponds to $c_a = 3$.
- Figure 5.** Convergence of genetic algorithm inversion. After 150 generations the minimum objective function value was decreased from 65.5 to 26.9.
- Figure 6.** Inversion result produced by the genetic algorithm. No regularization was applied and 150 generations were used. Many of the fine details may be artificial, especially in regions of sparse data coverage.
- Figure 7.** Comparison of depth to basement from gravity models in Figures 3b and 4b and shallow and deep Pz picks along REG-3 from Feighner et al. (1998). The shallow Pz picks from REG-3 are more consistent with the gravity models.

PRIOR MODEL

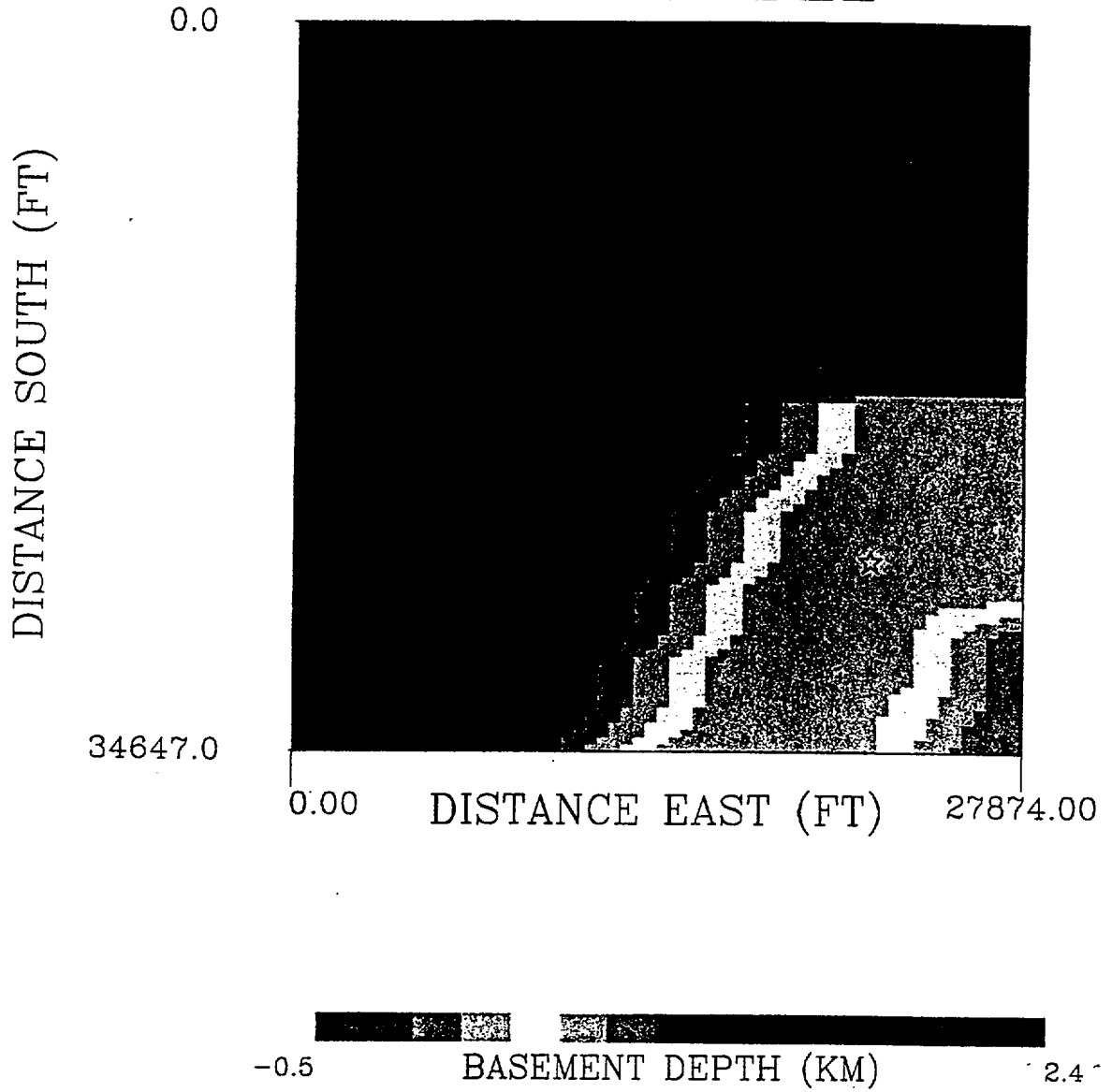


Figure 1.

YMP+USGS GRAVITY

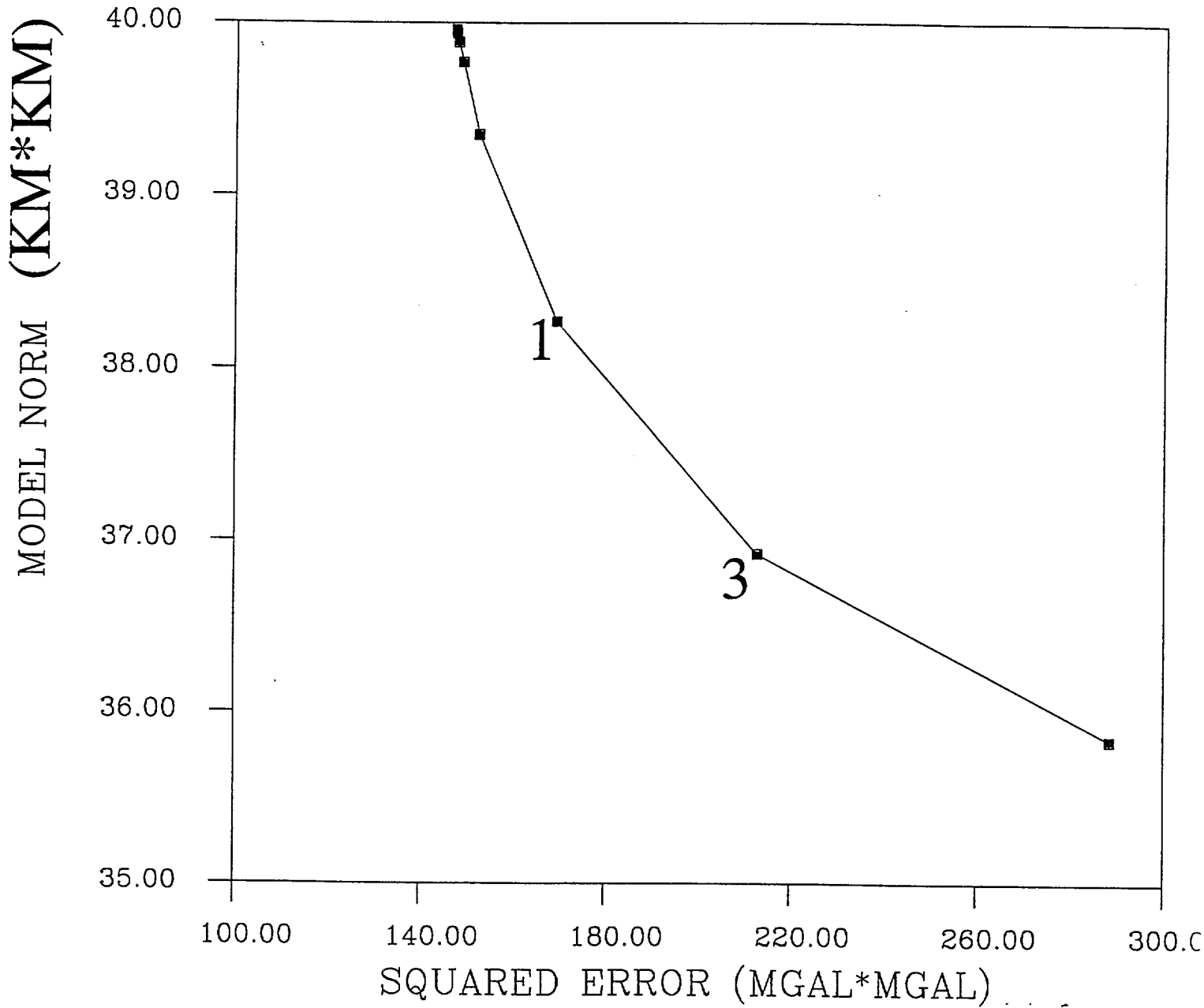


Figure 2.

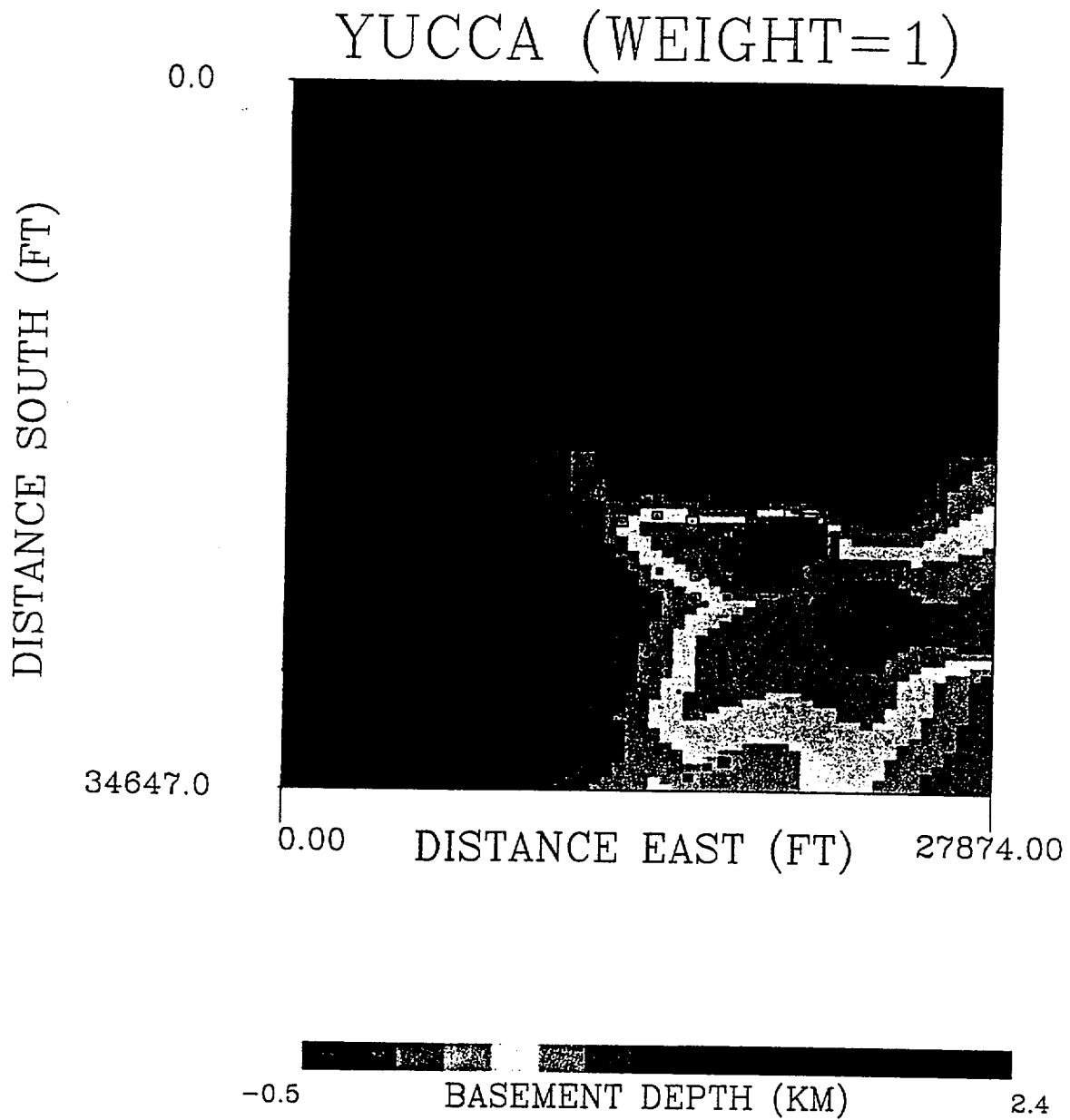


Figure 3a.

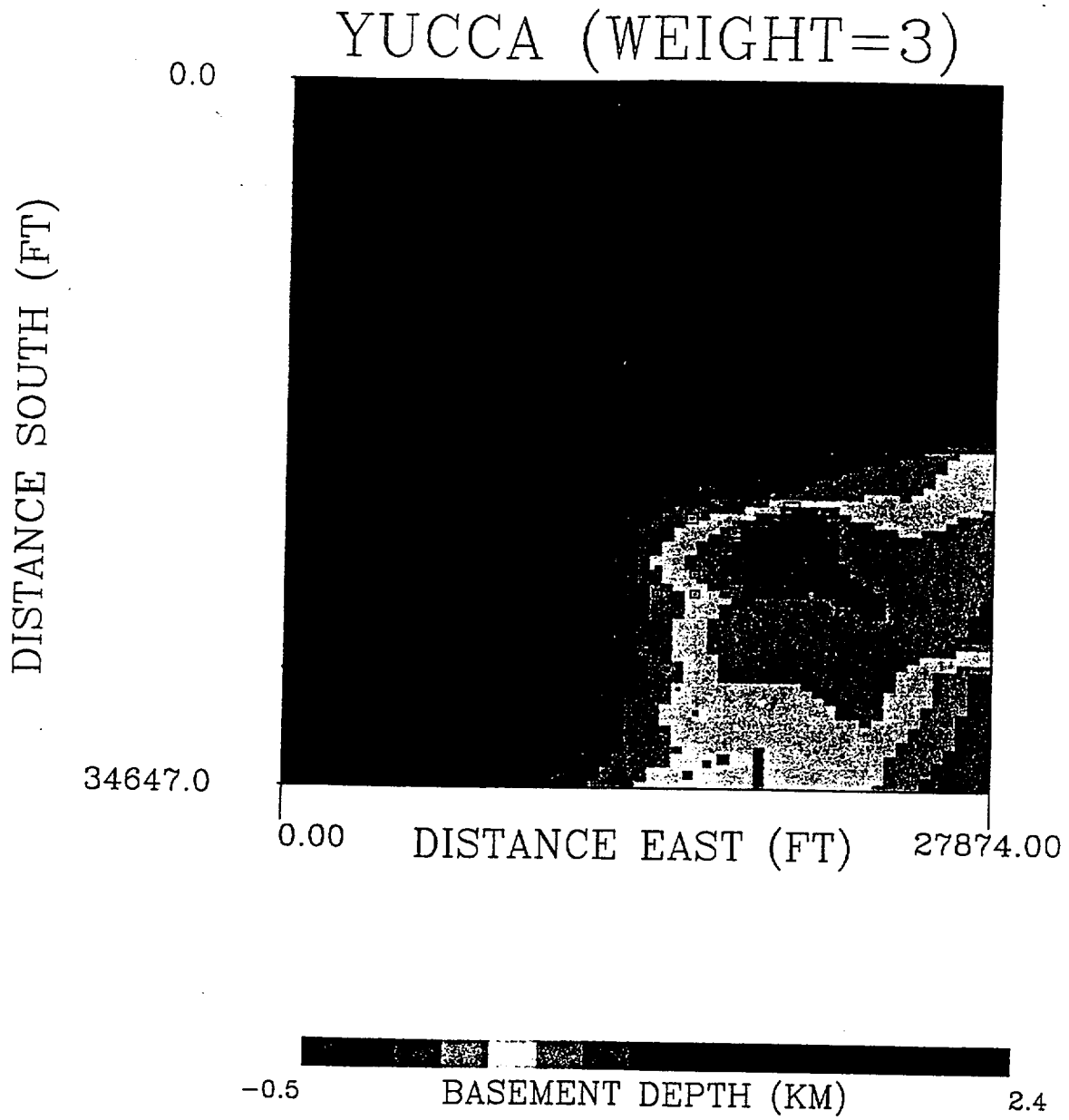


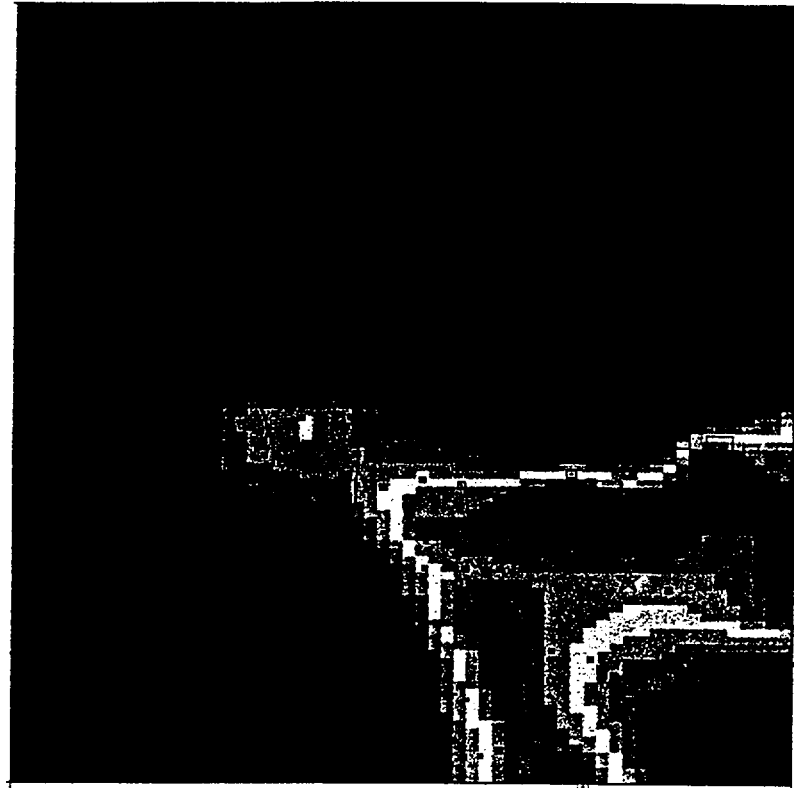
Figure 3b.

YUCCA+USGS (WEIGHT=1)

DISTANCE SOUTH (FT)

0.0

34647.0



0.00

DISTANCE EAST (FT)

27874.00

-0.5

BASEMENT DEPTH (KM)

2.4

Figure 4a.

YUCCA+USGS (WEIGHT=3)

DISTANCE SOUTH (FT)

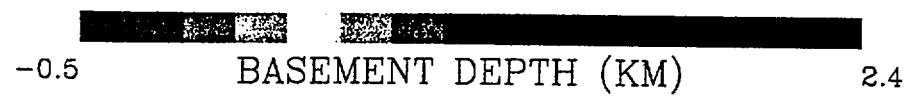
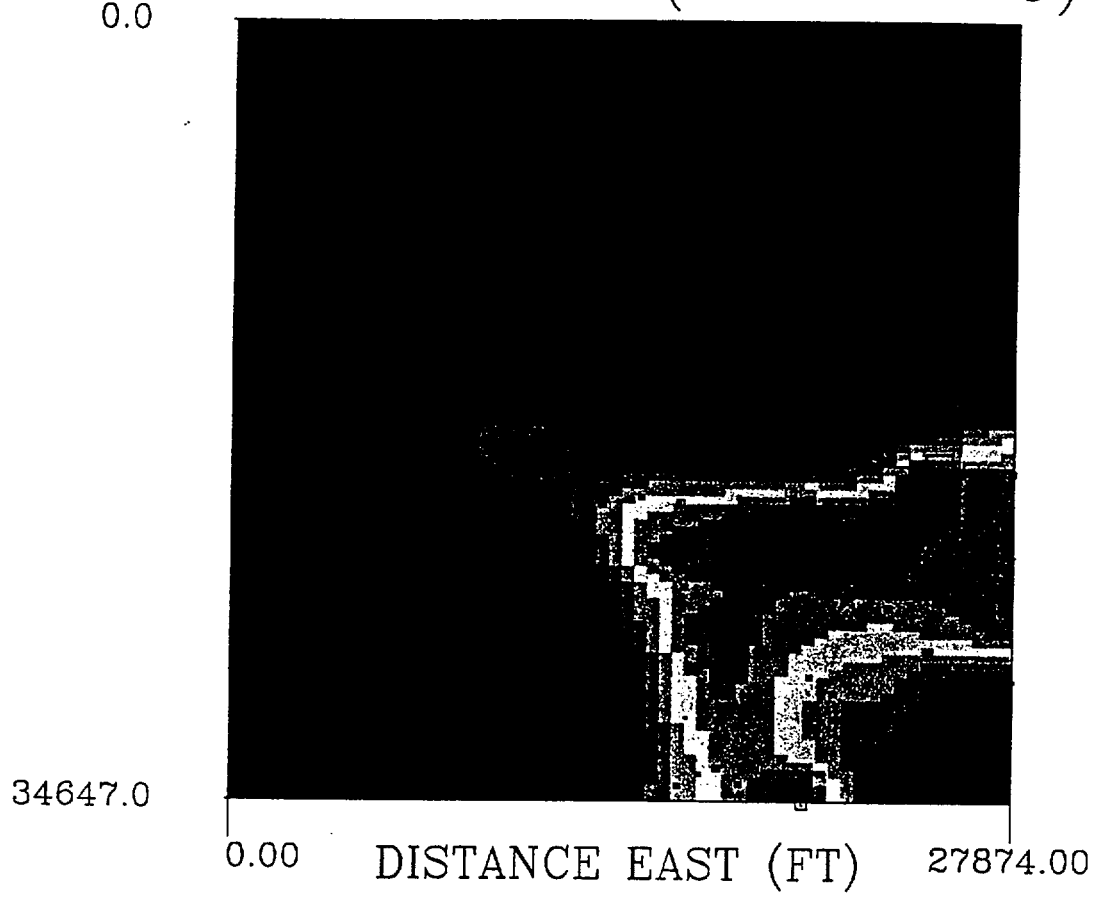


Figure 4b.

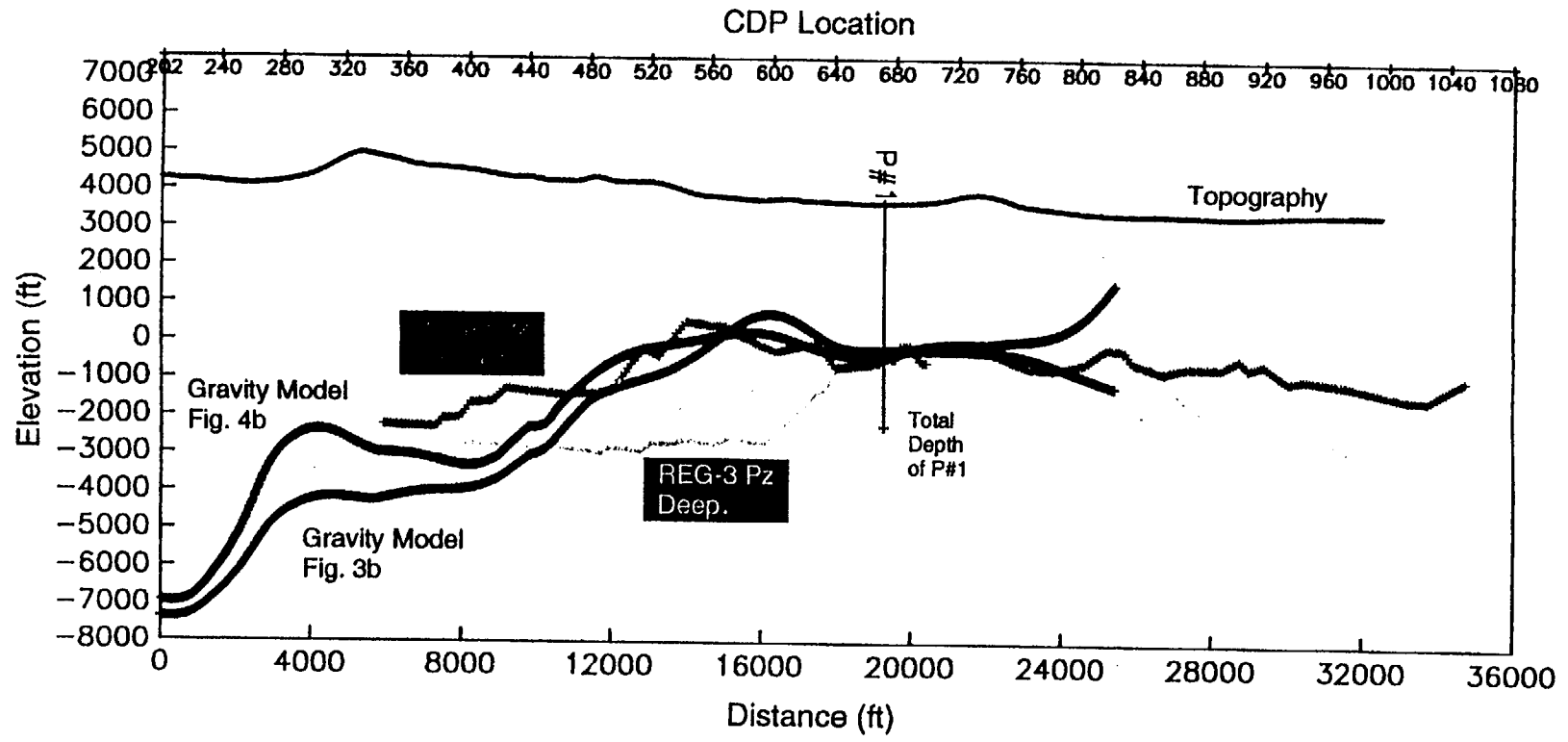


Figure 7.

YUCCA+USGS (GENETIC ALGORITHM)

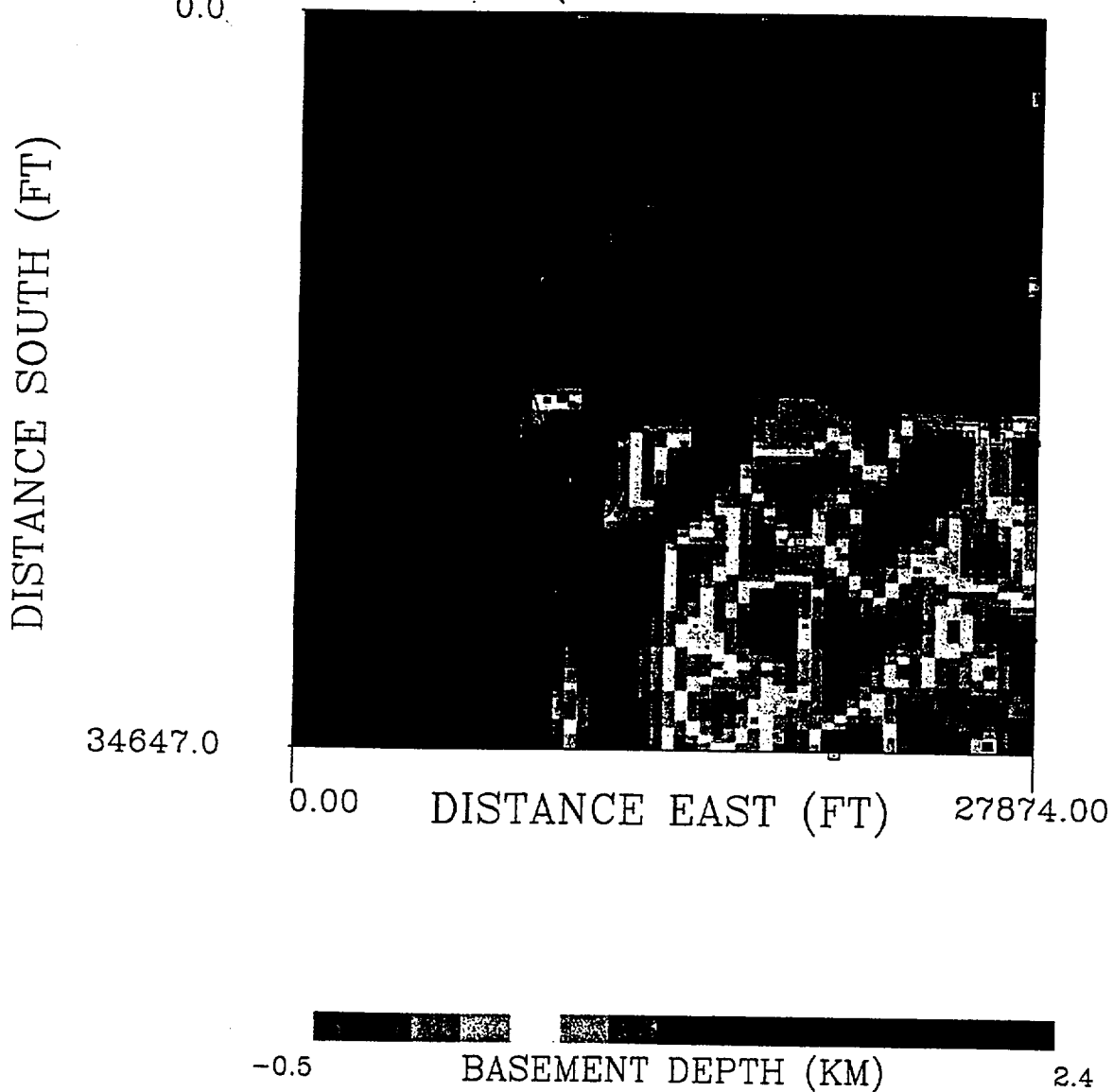


Figure 6.

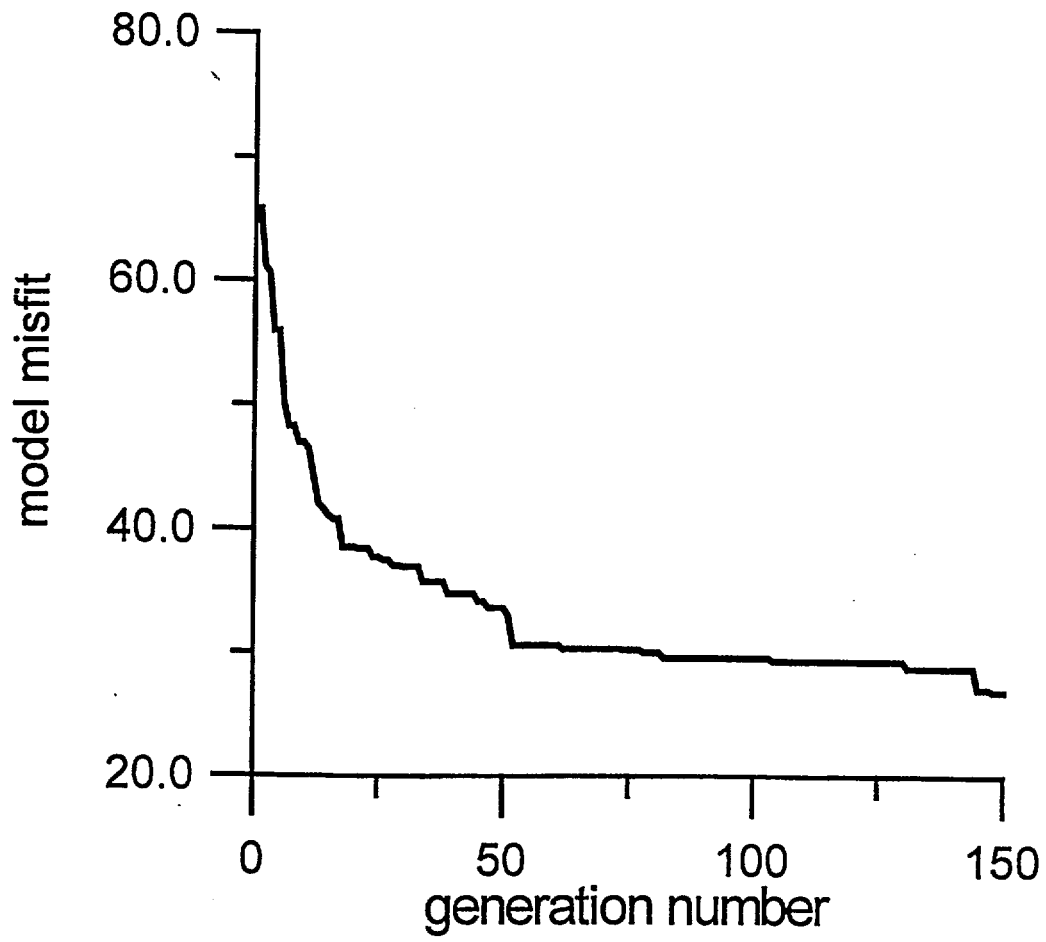


Fig. (5).